

Research Article

Geochemical Characteristics of Trace Elements and REEs and their Geological Significance for Uranium Mineralization within the Qianjiadian Sandstone-Hosted Uranium Deposit, Songliao Basin

Zhaobin Yan ^{1,2}, Hongjie Ji ^{1,3}, Guolin Guo ^{1,3}, Fei Xia,^{1,2} Wenwen Zhang,^{1,2} Saisai Song,^{1,2} and Shaofang Liu⁴

¹State Key Laboratory for Nuclear Resources and Environment, East China University of Technology, Nanchang 330013, China

²School of Earth Sciences, East China University of Technology, Nanchang 330013, China

³Fundamental Science on Radioactive Geology and Exploration Technology Laboratory, East China University of Technology, Nanchang 330013, China

⁴Key Lab of Bioprocess Engineering of Jiangxi Province, College of Life Sciences, Jiangxi Science and Technology Normal University, Nanchang 330013, China

Correspondence should be addressed to Hongjie Ji; a13875759760@126.com

Received 15 December 2022; Revised 1 April 2023; Accepted 10 April 2023; Published 20 April 2023

Academic Editor: Fan Yang

Copyright © 2023 Zhaobin Yan et al. This is an open access article distributed under the Creative Commons Attribution License, which permits unrestricted use, distribution, and reproduction in any medium, provided the original work is properly cited.

The Qianjiadian uranium deposit is a typical interstratified oxidized zone sandstone-hosted uranium deposit hosted in the Upper Cretaceous Yaojia Formation of the southern Songliao Basin. Despite its significance, little research has been conducted on the relationship between trace elements, REEs, and uranium mineralization in this deposit. This study presents new geochemical data from sandstones in the oxidation, transition, and reduction zones. The sandstones in the transition zone are highly enriched in U and moderately enriched in Mo, Cd, and V compared to those in the oxidation and reduction zones. They are also weakly enriched in Co, Ni, and Zn. The oxidation and transition zone sandstones have higher Σ LREE and Σ HREE contents than those in the reduction zone. However, the oxidation zone sandstones are characterized by LREE enrichment and flat HRRE distribution, while the transition zone sandstones show HRRE enrichment and flat LREE distribution. These trace element and REE differentiation characteristics within each subzone are closely related to the geological process of interstratified oxygenation. Oxygenated uranium-bearing fluids from southwestern provenance areas carried multiple trace elements and REEs and infiltrated along the oxidation sandstones to reach the Yaojia Formation's transition zone. During this process, a certain amount of Mo, V, Cd, and LREE from the oxygenated ore-forming fluids was precipitated by Fe-Mn hydroxide adsorption or calcite and siderite cementation. Meanwhile, about 20.33% of preexisting U in the oxidation zone sandstones was continuously extracted and entered into the oxygenated ore-forming fluids. In the transition zone, where dissolved oxygen was exhausted and hydrocarbons were continuously injected, U, Mo, Cd, V, Co, Ni, Zn, and REEs were unloaded and precipitated as uranium minerals, sulfide minerals, or carbonate minerals. The enrichment of Mo, Cd, V, and HREEs in the sandstones can serve as new prospecting indicators for the Qianjiadian uranium deposit.

1. Introduction

Sandstone-hosted uranium deposits are currently the most prospective and economic uranium resources for in situ leaching exploitation [1]. The formation of these deposits

is generally attributed to the reduction of U(VI) in oxygenated uranium-bearing groundwater to U(IV), resulting in uranium enrichment [2]. The Qianjiadian uranium deposit, located in the southern Songliao Basin (Figure 1), is considered a large interstratified oxidized zone sandstone-hosted

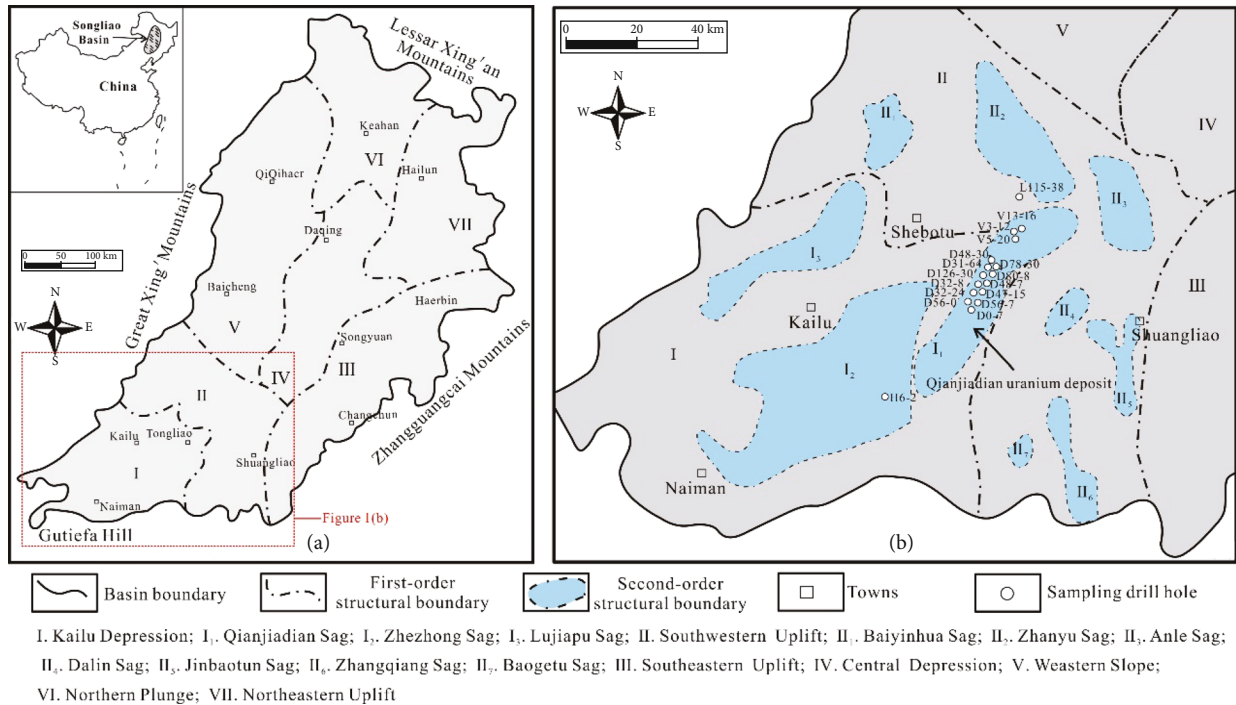


FIGURE 1: (a) Structural units of the Songliao Basin (modified from [6]). (b) Interior tectonic units of the southwestern Songliao Basin and sampling locations of the drill holes (modified from [5, 12]).

uranium deposit [3–8]. Its sandstones are further divided into oxidation, transition, and reduction zones based on redox conditions. The deposit is hosted in the Upper Cretaceous Yaojia Formation. The relationship between the distribution of the interstratified oxidized zone and sedimentary facies has been widely discussed in the Yaojia Formation [4, 7, 8]. Well-documented studies have focused on the occurrence state of uranium, metallogenic temperature, metallogenic fluid source, and metallogenic age involved in the uranium mineralization of the Qianjiadian deposit [9–15]. These characteristics were determined through petrographic observation, mineralogical analysis, inclusion salinity and temperature measurement, and U-Pb isotope dating [9–15]. Additionally, many studies have investigated the role of abiotic (e.g., pyrite and aqueous sulfides) and organic matter (e.g., microorganisms, carbonaceous debris, and hydrocarbons) as reductive agents of U(VI) to U(IV) in the Qianjiadian sandstone-hosted uranium deposit [5, 6, 13, 15]. Based on these researches, several ore-controlling factors and metallogenic models have been proposed in conjunction with the tectonic evolution history of the Songliao Basin [9, 14, 16, 17]. However, little attention has been paid to the geochemical behavior of trace elements and REEs within the interstratified oxidized zone sandstones. Previously, trace elements and REEs in Yaojia Formation sandstones were mainly used to reflect the rock composition and tectonic setting of the provenance [18, 19].

The aim of this study is to characterize the geochemistry of trace elements and REEs in sandstones from each subzone of the interstratified oxidized zone of the Yaojia Formation in the Qianjiadian uranium deposit. Based on this data, the

relationship between trace elements, REEs, and uranium mineralization will be discussed.

2. Geological Setting

The Songliao Basin is a large terrestrial basin located in northeast China. It was formed during the Late Mesozoic through Cenozoic and is one of the most important energy-producing basins in the world (Figure 1(a)). Geographically, it is surrounded by the Zhangguangcai Mountains to the southeast, the Lesser Xing'an Mountains to the northeast, the Great Xing'an Mountains to the northwest, and Gutiefa Hill to the south [20] (Figure 1(a)). The Zhangguangcai Mountains and Lesser Xing'an Mountains mainly consist of Late Triassic to Middle Jurassic magmatic rocks, while the Great Xing'an Mountains are composed of Late Paleozoic and Early Cretaceous granites and volcanic rocks [21]. The Songliao Basin can be subdivided into seven major structural units based on its basement morphology: the Kailu Depression, the Southwestern Uplift, the Western Slope, the Southeastern Uplift, the Northeastern Uplift, the Central Depression, and the Northern Plunge [19, 22] (Figure 1(a)).

The Qianjiadian uranium deposit is located in the Kailu Depression (Figure 1(b)). The basement of the Kailu Depression mainly consists of Precambrian to Paleozoic metamorphic and magmatic rocks, which are covered by Cretaceous, Paleogene, and Neogene sedimentary sequences with a maximum thickness of 5 km [19, 23]. The Kailu Depression was formed and filled in four main tectonic stages from the Cretaceous through the Neogene (Figure 2(a)). The first

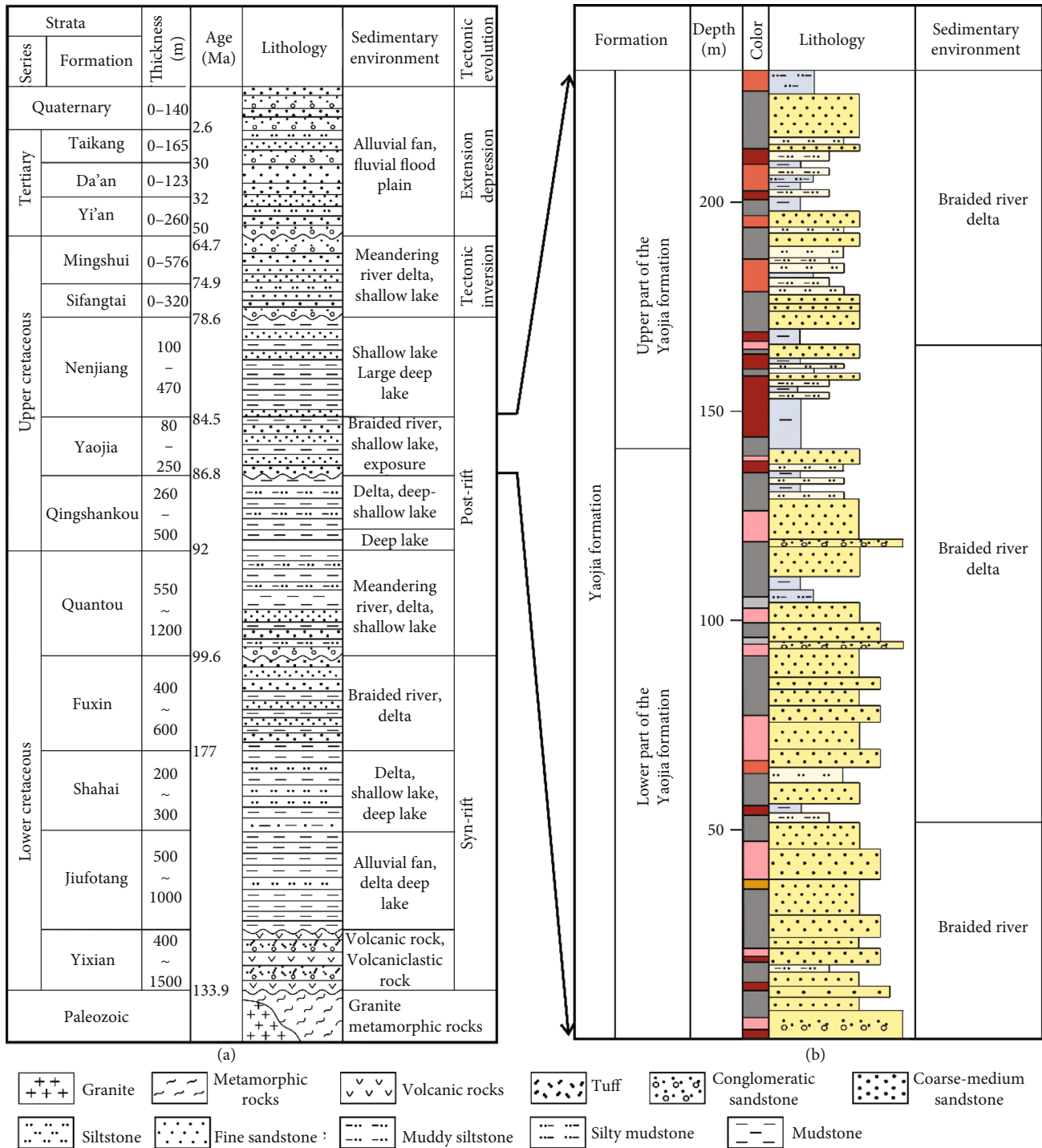


FIGURE 2: (a) Stratigraphic column and tectonic evolution phase of the southwestern Songliao Basin (modified from [13, 32-35]). (b) Stratigraphic column of the Yaojia Formation in the Qianjiadian uranium deposit (modified from [32]).

stage was a synrift stage during the Early Cretaceous that includes the Yixian, Jiufotang, Shahai, and Fuxin Formations. The Yixian Formation is represented by volcanoclastic and volcanic rocks, and the other Formations consist mainly of dark lacustrine fine-grained sediments, which contain abundant organic matter and are the main hydrocarbon source rocks of the basin [13, 24]. The second stage was a postrift thermal subsidence stage during the Late Cretaceous

that includes the Quantou, Qingshankou, Yaojia, and Nenjiang Formations. The Quantou and Yaojia Formations are mainly composed of deltaic and braided fluvial coarse-grained sediments, whereas there were two large-scaled lake transgressions occurred in the Qingshankou and Nenjiang Formations resulting in the formation of two sets of thick-bedded black mudstone as important regional caprocks [25]. The third stage was a tectonic inversion stage during

the end of the Late Cretaceous that includes the Sifangtai and Mingshui Formations, which are characterized by the fluvial and alluvial coarse-grained sediments [25, 26]. The fourth stage was an extension depression stage that occurred since the Paleogene and includes fluvial sediments of the Yi'an, Da'an, and Taikang Formations [27].

In the Qianjiadian uranium deposit, the uranium-ore-bearing Yaojia Formation mainly consists of red, yellow, and grey medium- to fine-grained arkosic and lithic sandstones, with red or grey mudstone and siltstone interlayers as aquitards [13] (Figure 2(b)). At the northeast of the Qianjiadian uranium deposit, the Yaojia Formation was tilted up during the end of the Late Cretaceous due to regional tectonic inversion and then denuded, resulting in the formation of a tectonic window [6, 28]. Oxygenated uranium-bearing fluids from the southwestern, northwestern, and southeastern mountains of the Kailu Depression infiltrated into and flowed along the sandstone layers of the Yaojia Formation [29]. The tectonic windows provided a discharge passage for confined groundwater [30]. Long-term oxidation and reduction of oxygenated uranium-bearing groundwater occurred in the sandstones of the Yaojia Formation, resulting in the formation of interstratified oxidized zone sandstone-hosted uranium deposits [3, 7]. The Qianjiadian uranium ore bodies are tabular or lenticular in shape and mainly occur in the sandstones of the lower Yaojia Formation [13].

The sandstones of the Yaojia Formation are generally weak in diagenesis and loose in cementation. They can be further divided into an oxidation zone, a transition zone, and a reduction zone based on their color, altered mineral assemblage, and degree of uranium mineralization [3–6, 27]. The oxidation zone mainly consists of red and yellow sandstones characterized by an alteration mineral assemblage of limonite and hematite [3, 31]. The transition zone is characterized by light grey or off-white sandstones with uranium mineralization that mainly occur near the front line of the oxidation zone. In the sandstones of the transition zone, uranium exists in the form of uranium minerals and adsorbed uranium. Uranium minerals are dominated by pitchblende, coffinite, and brannerite [1, 6, 14]. Uranium in the adsorbed state is mainly adsorbed by clay minerals such as kaolinite, illite, and montmorillonite [14, 15]. Epigenetic minerals including sulfide and carbonate minerals are common in the transition zone [14]. The reduction zone is represented by primary grey sandstones with nonmineralization. The ratios of oxidized sandstones in the Yaojia Formation decrease from the periphery to the center [32].

3. Materials and Methods

Ninety-two sandstone samples were collected from seventeen drill holes located in the Qianjiadian Sag of the Kailu Depression (Tables S1, S2; Figure 1(b)). These drill holes were finished in the Yaojia Formation, and the whole interval coring of the Yaojia, Nenjiang, Sifangtai, and Mingshui Formations was carried out. During the sampling process, gamma-ray responses were measured using an HD-2000 gamma radiometer to roughly distinguish the degree of

uranium mineralization. All sandstone samples were classified into three categories based on their color and gamma-ray responses. The first type of sandstone samples is from the oxidation zone and is red or yellow in color. There are a total of 52 samples of this type. The second type is from the transition zone and is light grey or off-white in color. These samples have high gamma-ray response values and more plant carbon debris, with a total of 26 samples. The third type is from the reduction zone and is dark grey or grey in color. These samples have low gamma-ray response values, and there are a total of 14 samples.

All samples were analyzed for bulk-rock trace element and REE at Wuhan Sample Solution Analytical Technology Co., Ltd. in Wuhan, China. The samples were milled to a powder with a 200 mesh size and dried in an oven at 105°C for 12 hours. Each sample was weighed to 50 mg and placed in a Teflon vial. Then, 1 ml of HNO₃ and 1 ml of HF were added to the vial in turn. The vials were placed in stainless steel sleeves and heated in an oven at 190°C for 24 hours. Afterward, the vials were opened and evaporated to dryness on a hotplate at 150°C. Later, 1 ml of HNO₃ was added and dried again. One milliliter of high purity HNO₃, 1 ml of H₂O, and 1 ml of an internal standard solution of In with a concentration of 1 ppm were added to the Teflon vials. The vials were then resealed and heated again in an oven at 190°C for more than 12 hours. After cooling, the solution of each sample was diluted to 100 g with 2% HNO₃. The final sample solutions were analyzed using an Agilent 7700e ICP-MS [36]. Mixed pure elemental standards were used as external standards to establish standard curves for each element. Standard samples of GSR-1 (granite), GSR-2 (andesite), and GSR-3 (basalt) were processed and tested together with the samples as reference materials [37]. The analytical uncertainties are less than 2% for most trace elements.

4. Results

4.1. Trace Element Geochemistry. The trace element contents of the Yaojia Formation sandstone samples are displayed in Table S1. Sedimentary rocks are known for their heterogeneity, and their material composition may vary greatly. Estimating the relative enrichment or depletion of trace elements in sandstones between each zone based solely on their absolute content may result in deviation. This deviation may not be related to later geological fluid action, such as the dilution effect caused by plant carbonaceous or biogenic carbonate rocks. In the supergene environment, the Th element has only one valence state (+4) and is insoluble, making it a relatively inert trace element. The average content of Th in the sandstones of the reduction zone, oxidation zone, and transition zone in this study is 7.77 ppm, 7.77 ppm, and 7.95 ppm, respectively (Table S1), indicating that Th is very stable. Therefore, Th is used to standardize the trace elements of all samples for comparison in this study. The enrichment factor (EF) is used to express the degree of enrichment or depletion of trace elements. The relative enrichment factor of element X

between two geological units can be expressed as $EF X = (X1/Th1)/(X2/Th2)$ [38]. By comparing the average value of trace elements in samples from the transition zone and oxidation zone with that of sandstones in the reduction zone, the enrichment factors of each element are obtained (Table 1 and Figure 3). The enrichment factors of the transition zone relative to the oxidation zone are also obtained (Table 1 and Figure 3).

In this study, an element with a change rate of less than $\pm 10\%$ is considered stable and without migration during the process of interstratified oxygenation. An element with an enrichment factor greater than 1.1 is considered enriched, while an element with an enrichment factor less than 0.9 is considered deficient. An element with an enrichment factor between 1.1 and 0.9 is considered unchanged. Compared to the oxidation zone sandstones, the transition zone sandstones are highly enriched in U; moderately enriched in Mo, Cd, and V; weakly enriched in Co, Ni, Zn, and Sr; and slightly depleted in Li, Cu, and Ba. Other elements are relatively stable. In contrast, compared to the reduction zone sandstones, the transition zone sandstones are highly enriched in U; moderately enriched in Mo, Cd, and V; and weakly enriched in Co, Ni, and Zn. Other elements are relatively stable. The enrichment factors of the oxidation zone relative to the reduction zone show that most trace elements are relatively stable. Sr and U are slightly depleted, while V, Cd, Ba, and Mo are weakly enriched to varying degrees.

4.2. REE Geochemistry. The REE content of the samples is listed in Table S2. The $\sum REE$ content in oxidation zone sandstones ranges from 72.66 ppm to 185.56 ppm with an average of 126.13 ppm. This is approximately equal to that of the transition zone sandstones, which range from 99.97 ppm to 186.32 ppm with an average of 127.38 ppm. Both are higher than that of the reduction zone sandstones, which range from 99.49 ppm to 139.68 ppm with an average of 117.18 ppm. The average value of the $\sum LREE$ content of sandstones in the transition zone is identical to that of sandstones in the oxidation zone. The average value of the $\sum HREE$ content of sandstones in the transition zone is higher than that of sandstones in the oxidation zone. The $\sum LREE/\sum HREE$ ratios of sandstones in the oxidation zone, transition zone, and reduction zone are 5.92~12.43 (average 9.09), 2.2~10.35 (average 8.53), and 7.68~10.40 (average 8.55), respectively. The average ratios of $(La/Yb)_N$, $(La/Sm)_N$, and $(Gd/Yb)_N$ for sandstones in the oxidation zone are 9.25, 4.13, and 1.36, respectively. For sandstones in the transition zone, they are 8.70, 3.92, and 1.37, respectively. For sandstones in the reduction zone, they are 8.72, 3.98, and 1.35, respectively. The Yaojia Formation sandstones show obvious LREE enrichment and HREE depletion. The chondrite-normalized REE distribution patterns among samples from the oxidation zone, transition zone, and reduction zone are consistent with the upper crust (Figure 4). This indicates that the interstratified oxidized zone of the Qianjiadian uranium deposit has not been reformed by deep fluids. All samples display a similar negative Eu anomaly (δEu)

TABLE 1: Enrichment factor (EF) of trace element for sandstones in the Qianjiadian uranium deposit.

Element	EF of oxidation zone relative to reduction zone	EF of transition zone relative to reduction zone	EF of transition zone relative to oxidation zone
Li	1.03	0.89	0.87
Be	1.09	1.10	1.02
Sc	1.07	1.10	1.03
V	1.25	2.23	1.79
Co	1.01	1.15	1.14
Ni	1.01	1.19	1.19
Cu	1.03	0.90	0.88
Zn	0.92	1.14	1.24
Ga	1.05	1.08	1.03
Rb	1.05	1.04	0.99
Sr	0.85	1.02	1.20
Zr	1.00	0.97	0.97
Nb	0.99	0.96	0.97
Mo	1.21	7.69	6.36
Cd	1.12	3.92	3.50
Sn	1.00	1.01	1.01
Ba	1.15	0.99	0.86
Hf	1.01	0.95	0.93
Ta	1.00	1.02	1.02
Th	1.00	1.00	1.00
U	0.81	47.71	58.80

with a mean value of 0.59~0.62, which is lower than that of UCC (0.71).

5. Discussion

5.1. Geochemical Behavior Analysis of the Trace Elements

5.1.1. Uranium (U). In oxygenated uranium-bearing fluids, the U element is usually hexavalent in the form of UO_2^{2+} , which generally combines with carbanions to form $[UO_2(CO_3)_2]^{2-}$. Under a sulfate-reducing environment, similar to the transition from Fe(III) to Fe(II), U(VI) is reduced to U(IV), causing the formation of uranium minerals or precipitation in the form of hydroxyl complexes with high surface activity [40, 41]. This results in the enrichment of the U element in sedimentary rocks. The content of the U element in sandstones from the oxidation zone within the study area is the lowest, ranging from 0.96 ppm to 8.65 ppm with an average of 2.9 ppm. The U content of samples from the transition zone varies widely from 9.65 ppm to 2132.01 ppm with an average of 173.23 ppm. The U content of sandstone samples from the reduction zone varies from 1.14 ppm to 7.10 ppm with an average of 3.64 ppm (Table S1).

In this study, we found that the enrichment factor of uranium (U) in the oxidation zone relative to the reduction zone is 0.81 (Table 1 and Figure 3), indicating a depletion. This suggests that some pre-enriched uranium in the

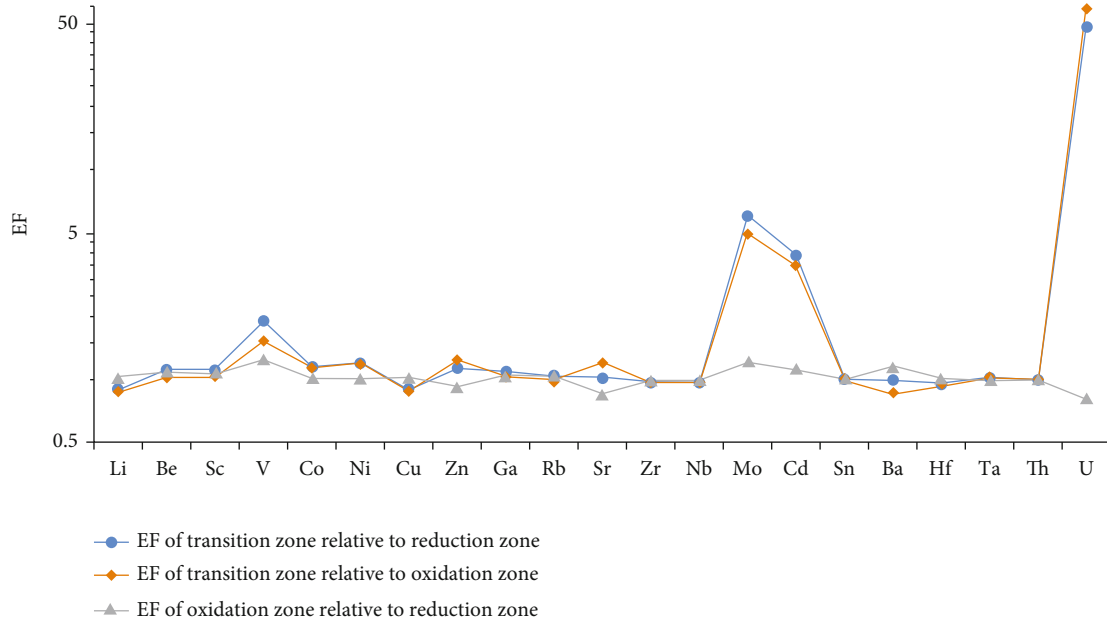


FIGURE 3: Relative enrichment factor (EF) of trace elements in the sandstones of Qianjiadian uranium deposit.

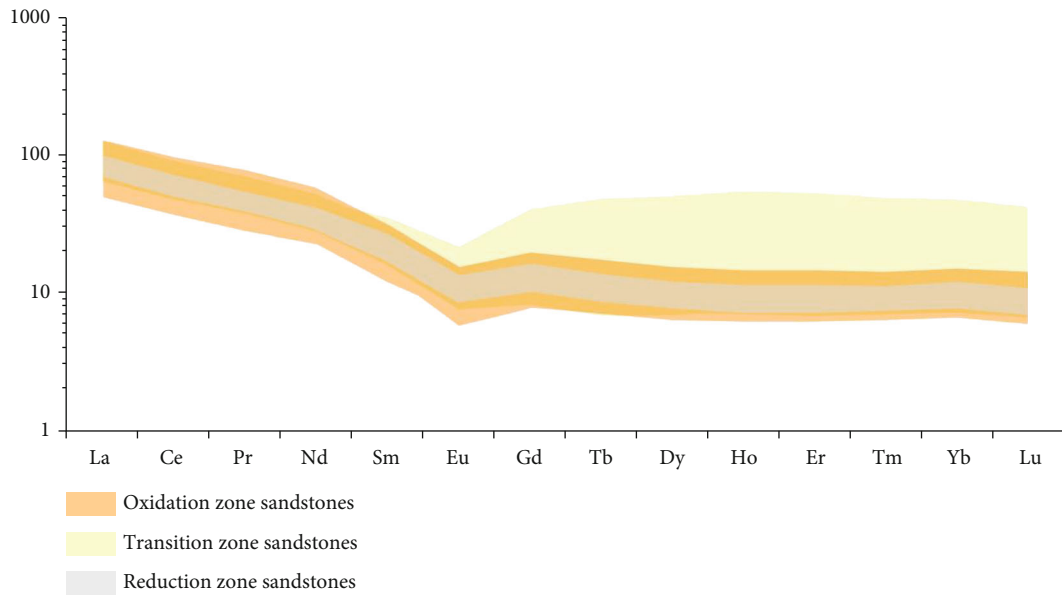


FIGURE 4: Chondrite-normalized REE patterns of the sandstones in the Qianjiadian uranium deposit, chondrite values from [39].

sandstones of the oxidation zone was continuously extracted under oxidation conditions. The pre-enriched uranium is believed to have mainly existed within clay minerals, Fe-Ti oxides, and uranium-rich lithic fragments [1, 13, 15] and was reactivated by transforming from U(IV) to U(VI). The leaching ratio of uranium (U) in the oxidation zone sandstone can be calculated using the equation: $R_{\text{extracting}} = (C_{\text{reduction}} - C_{\text{oxidation}}) / C_{\text{reduction}} \times 100\%$. Our study shows that 20.33% of the pre-enriched uranium in the oxidation zone sandstones was leached and entered into the ore-forming fluids, which infiltrated along the permeable layer

to reach the transition zone. In the transition zone, where dissolved oxygen had been exhausted and hydrocarbons had been injected [5, 13], U(VI) was reduced to U(IV), forming uranium minerals such as pitchblende and coffinite [1, 6, 14]. Additionally, with a uranium enrichment factor of 47.71 in the transition zone relative to the reduction zone (Table 1 and Figure 3), the uranium content is much higher than that of depleted uranium in the oxidation zone. Therefore, we speculate that most of the uranium in the Qianjiadian uranium deposit came from uranium-bearing source rocks in the basin marginal provenance areas.

5.1.2. Molybdenum (Mo). In the Yaojia Formation of the Qianjiadian uranium deposit, the molybdenum (Mo) content in the sandstones of the oxidation zone ranges from 0.33 ppm to 1.33 ppm, with an average of 0.56 ppm. However, the Mo content in sandstone samples from the transition zone varies significantly, ranging from 0.37 ppm to 30.87 ppm, with an average of 2.68 ppm (Table S1). In contrast, the Mo content in the reduction zone varies only slightly, ranging from 0.24 ppm to 0.76 ppm, with an average of 0.46 ppm. The enrichment factor of molybdenum (Mo) in the oxidation zone relative to the reduction zone is 1.21 (Table 1 and Figure 3), indicating a slight enrichment. However, in the transition zone relative to the reduction zone, the enrichment factor of Mo is 7.69 (Table 1 and Figure 3), indicating a moderate enrichment and making it the most enriched trace element after uranium (U).

Oxygenated meteoric water leached molybdenum-rich minerals from the source rocks in the provenance areas and oxidized Mo(IV) to Mo(VI), forming mainly molybdates (i.e., MoO_4^{2-}) under weakly acidic or neutral conditions [42]. These highly soluble molybdates were dissolved in the oxygenated ore-forming fluids and then permeated into the sandstones of the Yaojia Formation. Molybdenum (Mo) does not typically accumulate in organisms and has a weak affinity with minerals such as clay, carbonate, and Fe hydroxide [43]. However, under oxidation conditions, Mo is easily adsorbed by Mn hydroxide [44, 45]. Therefore, the slight enrichment of Mo in the oxidation zone relative to the reduction zone may be due to the capture of MoO_4^{2-} from oxygenated ore-forming fluids by the surface of Mn hydroxide. In the transition zone of the Qianjiadian uranium deposit, sulfates in the ore-forming fluids were reduced to sulfides such as pyrite, creating a strong sulfurization environment [13]. In this environment, MoO_4^{2-} was prone to being transformed into $\text{Mo}(\text{O}_x, \text{S}_{4-x})^{2-}$ or into Fe-Mo-S cluster complexes [45, 46]. $\text{Mo}(\text{O}_x, \text{S}_{4-x})^{2-}$ was then precipitated and fixed by combining with sulfur-rich organic molecules, iron-sulfide, and/or metal-rich particulate matter such as pyrite and uranium minerals [46], potentially resulting in the moderate enrichment of Mo in the transition zone. Electron probe analysis results from this study area show that the authigenic pyrite in the sandstones of the transition zone has a high Mo content, with an average value of 0.5%. Additionally, Mo content is positively correlated with U content (Figure 5(a)).

5.1.3. Cadmium (Cd). The distribution of cadmium (Cd) content in the sandstones of the oxidation and reduction zones is similar, both ranging from 20 ppb to 90 ppb, with average values of 45.7 ppb and 42.3 ppb, respectively. However, the range of Cd content in transition zone samples is significantly larger, ranging from 30 ppb to 2340 ppb, with an average of 170 ppb (Table S1). Of all the trace elements analyzed, Cd has the lowest content. In the transition zone relative to the reduction zone, the enrichment factor of Cd is 3.92, indicating a moderate enrichment (Table 1 and Figure 3). Compared to the reduction zone, the enrichment factor of cadmium (Cd) in the oxidation zone is 1.12, indicating a slight enrichment. The increased Cd in the

sandstones of the transition zone was mainly derived from the basin marginal provenance areas.

As a typical chalcophile element, cadmium (Cd) is also a sulfophile element like zinc (Zn) and has relatively unique geochemical behavior [47]. In provenance areas, Cd mainly exists in isomorphism with sphalerite and wurtzite. Under the action of oxygenated meteoric precipitation, Cd-containing minerals in source rocks such as sphalerite are prone to dissolution and oxidation [47], forming oxides such as CdO or CdSO_4 that enter oxygenated ore-forming fluids for relatively long-distance transport along permeable sandstones. Polarizing microscope and scanning electron microscope observations show that carbonate cements including dolomite, ankerite, calcite, and siderite are developed in the sandstones of the oxidation and transition zones of the Yaojia Formation [12, 14, 48]. Hydrocarbons from the source rocks of the Jiufotang (K1j) Formation acted as reductants [5, 9], generating a large amount of CO_2 that was expected to participate in carbonate cementation [13]. An alkaline environment was conducive to the precipitation of CdSO_4 in the form of otavite (CdCO_3) [47]. Meanwhile, the strong sulfurization environment in the transition zone was prone to transforming CdSO_4 into CdS (greenockite). Otavite and siderite have similar chemical properties and forming conditions and often occur as paragenetic minerals [47]. The siderite content in the transition and oxidation zones of the Qianjiadian uranium deposit was both low but approximately equal [48]. However, the degree of cadmium enrichment in the transition zone is much higher than that in the oxidation zone. Notably, there is a positive correlation between Cd and U content in the sandstones of the transition zone (Figure 5(b)), indicating that cadmium in the transition zone may be mainly fixed in the form of greenockite.

5.1.4. Vanadium (V). Under oxidation conditions, pentavalent vanadium generally occurs in the form of vanadate (VO_4^{3-} or VO_3^-), which is highly soluble in oxygen-containing fluids. Vanadate in groundwater can also be adsorbed by Fe-Mn hydroxides and kaolinite [49]. In reducing environments, V(V) can be reduced to V(IV), forming VO^{2+} , or to V(III), forming oxide V_2O_3 or hydroxide $\text{V}(\text{OH})_3$ [50, 51].

In the Yaojia Formation of the study area, the vanadium (V) content in the sandstones of the oxidation zone ranges from 14.79 ppm to 112.38 ppm, with an average of 39.76 ppm. The range of V content in sandstones from the transition zone is wider, ranging from 14.32 ppm to 268.78 ppm, with an average of 57.4 ppm (Table S1). The V content in sandstones from the reduction zone varies only slightly, ranging from 16.65 ppm to 55.15 ppm, with an average of 31.58 ppm. The enrichment factor of V in the oxidation zone relative to the reduction zone is 1.25 (Table 1 and Figure 3), indicating a slight enrichment. This may be similar to the reason for Mo enrichment in the oxidation zone: vanadate derived from the basin's southwestern source rocks was dissolved into oxygenated meteoric groundwater, and a portion was adsorbed by Fe-Mn hydroxide in the sandstones, resulting in V enrichment in the oxidation zone.

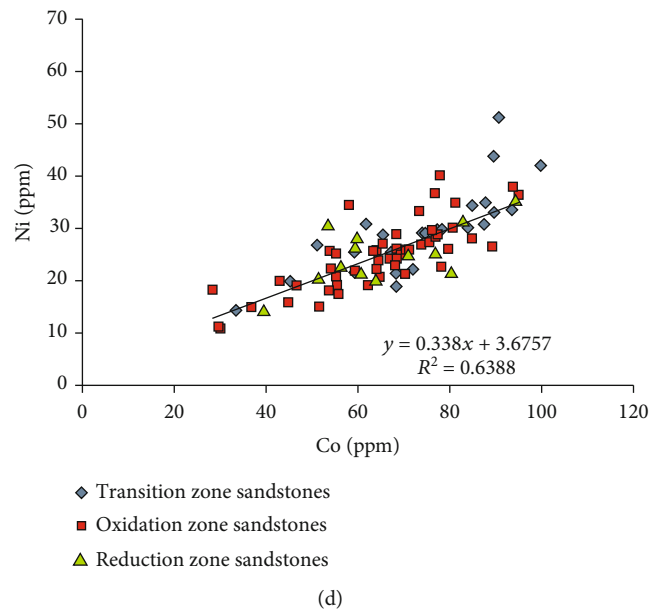
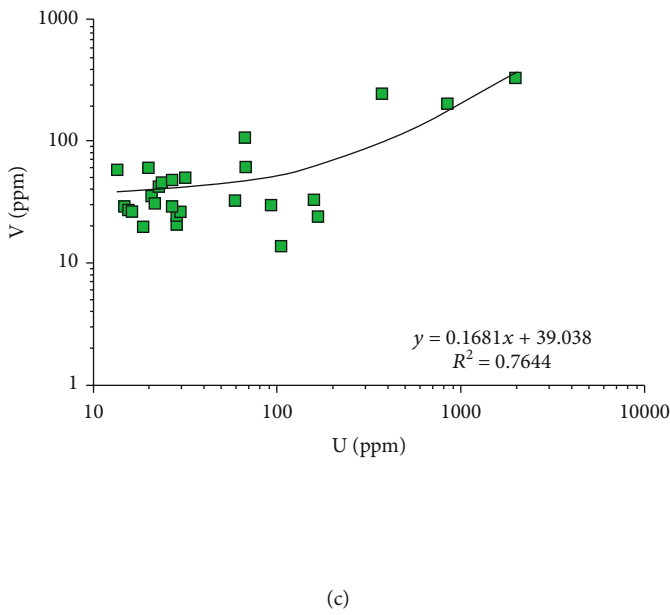
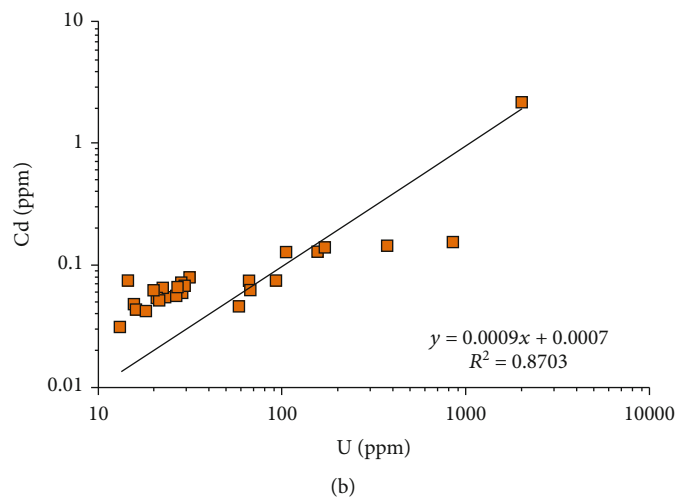
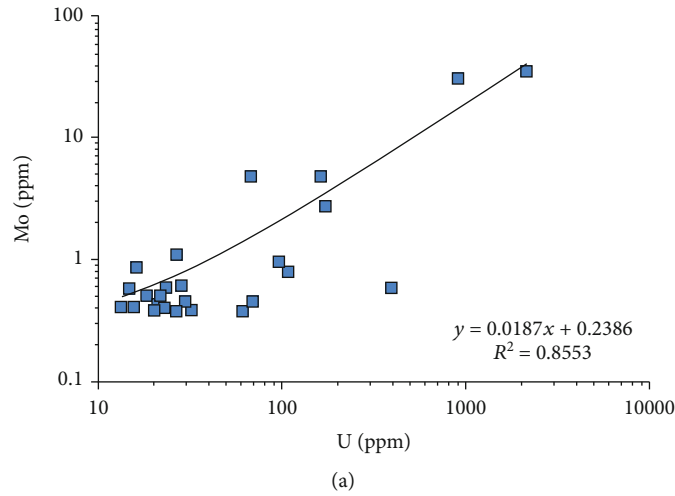


FIGURE 5: Continued.

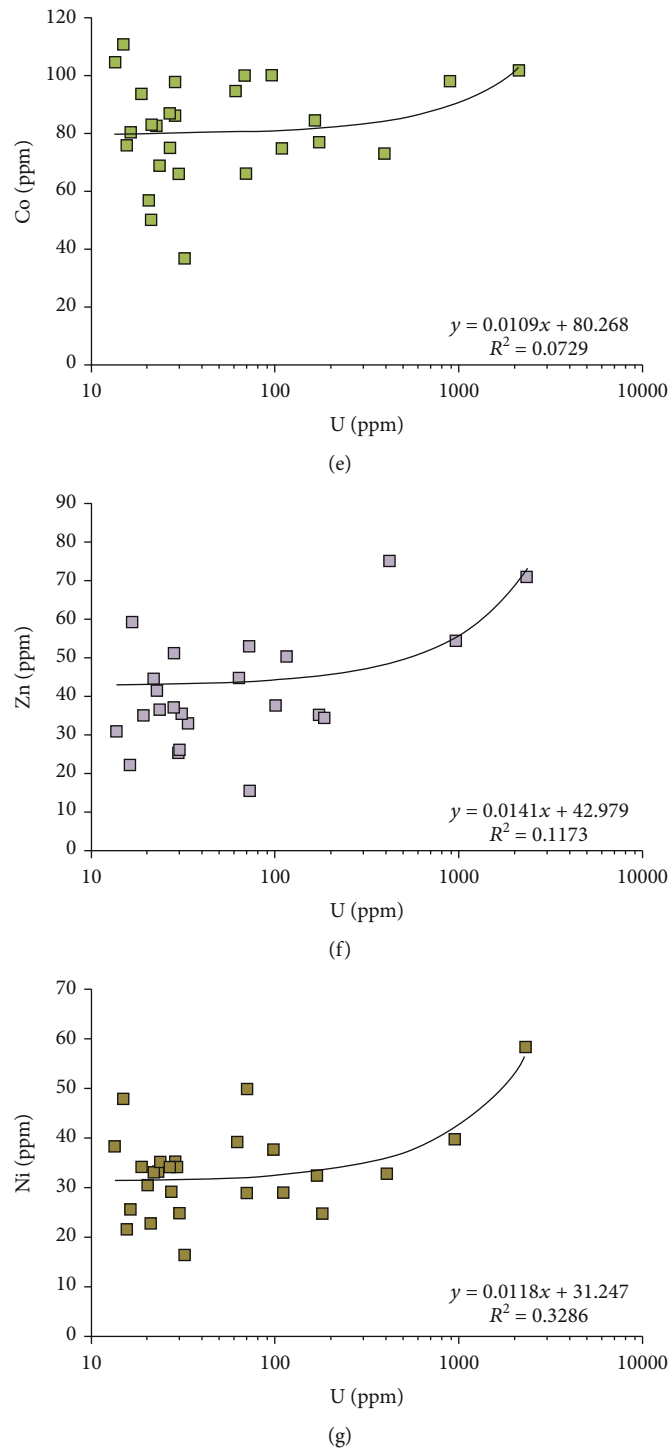


FIGURE 5: (a) Cross-plot of U content against Mo content of the sandstones in the transition zone. (b) Cross-plot of U content against Cd content of the sandstones in the transition zone. (c) Cross-plot of U content against V content of the sandstones in the transition zone. (d) Cross-plot of Co content against Ni content of the sandstones in Qianjiadian uranium deposit. (e) Cross-plot of U content against Co content of the sandstones in the transition zone. (f) Cross-plot of U content against Zn content of the sandstones in the transition zone. (g) Cross-plot of U content against Ni content of the sandstones in the transition zone.

Furthermore, in the transition zone relative to the reduction zone, the enrichment factor of vanadium (V) is 2.23, indicating a moderate enrichment (Table 1 and Figure 3). The total sulfur content in the sandstones of the transition

zone is high, with an average value of 1.85% [52], and abundant authigenic pyrite is present [3, 5, 10, 14], indicating a strong reducing environment. It is assumed that the remaining vanadate in the ore-forming fluids passing

through the oxidation zone was reduced to V_2O_3 or $V(OH)_3$ here and precipitated together with uranium minerals. As a result, V content is positively correlated with U content (Figure 5(c)).

5.1.5. Cobalt (Co), Nickel (Ni), and Zinc (Zn). In the oxidation, transition, and reduction zones of the Yaojia Formation of the Qianjiadian uranium deposit, the average values of cobalt (Co) content are 73.52 ppm, 82.15 ppm, and 73.79 ppm, respectively. The average values of nickel (Ni) content are 28.73 ppm, 33.28 ppm, and 28.41 ppm, respectively. The average values of zinc (Zn) content are 39.30 ppm, 45.42 ppm, and 40.43 ppm, respectively (Table S2). In this study, Co content shows a good linear correlation with Ni content (Figure 5(d)). The enrichment factors of cobalt (Co), nickel (Ni), and zinc (Zn) in the oxidation zone relative to the reduction zone are close to 1. In contrast, the enrichment factors of the transition zone relative to the reduction zone are 1.15, 1.19, and 1.14, respectively (Table 1 and Figure 3), indicating a slight enrichment. Co, Ni, and Zn from source rocks in provenance areas were able to be leached and dissolved into oxygen-rich groundwater in the form of divalent ions or $CoCl^+$, $NiCl^+$, and $ZnCl^+$ [53]. Cobalt (Co), nickel (Ni), and zinc (Zn) are sulfophile elements. Under the sulfate-reducing conditions of the transition zone, Co^{2+} , Ni^{2+} , and Zn^{2+} from ore-forming fluids were apt to form insoluble sulfides such as CoS, NiS, and $[Zn, Fe]S$, which precipitated together with authigenic pyrite as solid solutions [54]. Both Co and Zn contents are weakly correlated with U content since their Pearson correlation coefficients are less than 0.2 (Figures 5(e) and 5(f)). Ni content is weakly correlated with U content (Figure 5(g)).

5.2. Geochemical Behavior Analysis of the REEs. The mobility of rare earth elements (REEs) in water-rock interactions has been a subject of debate. Some researchers believe that REEs can be activated in various water-rock reaction processes [55]. However, others believe that REEs are not active in low-temperature ($<350^\circ C$) water-rock reactions, such as diagenesis, and have no influence on the REE composition of sediments [56]. In this study, the $\sum REE$ content in the sandstones of the oxidation and transition zones of the Qianjiadian uranium deposit is significantly higher than that in the reduction zone. The increase in $\sum REE$ content may be due to the introduction of oxygenated ore-forming fluids from erosion source areas. Additionally, $\sum REE$ and $\sum LREE$ contents are weakly correlated with U content (Figures 6(a) and 6(b)), while $\sum HREE$ content shows a positive correlation with U content in the transition zone (Figure 6(c)). To better reflect the mobility of REEs in the uranium mineralization process, the average values of REE content in reduction zone sandstones were used as a standard to normalize REEs in oxidation and transition zone sandstones. Relative to reduction zone sandstones, oxidation and transition zone sandstones show similar degrees of LREE enrichment but distinctly different degrees of HREE enrichment (Figure 7). The distribution pattern of REEs in the oxidation zone sandstones is

right-leaning, with an enrichment of LREEs and a depletion of HREEs. In contrast, the distribution pattern in the transition zone sandstones is left-leaning, with an enrichment of HREEs and a flat distribution of LREEs (as shown in Figure 7). These characteristics suggest that REEs are active under low-temperature groundwater conditions and that HREEs are more likely to migrate than LREEs during the process of uranium mineralization.

REE ions, which resemble uranyl ions (UO_2^{2+}), are alkaline cations that can combine with carbanions, chloride ions, and sulfate ions to form stable soluble complexes under acidic conditions. This is especially true for fluids rich in carbanions, which can more easily migrate REEs [56, 57]. The main carbonate complex of REEs in soil solution is $[REE(CO_3)_2]^-$, with HREEs being more likely to form $[REE(CO_3)_2]^-$ than LREEs [53]. In the Yaojia Formation sandstones of the Qianjiadian uranium deposit, carbonate cements consist of dolomite, siderite, ankerite, and calcite [12, 14, 48]. XRD analyses show that the average content of carbonate cements in sandstones from the transition zone, oxidation zone, and reduction zone is 14.27%, 13.33%, and 3.89%, respectively [48]. The content of $\sum REE$ also decreases gradually from the transition zone to the oxidation zone and then to the reduction zone in this study. There is a positive correlation between the content of $\sum REE$ and the content of carbonate cement. This suggests that $[REE(CO_3)_2]^-$ from infiltrated groundwater may precipitate along with carbonate cements in the transition and oxidation zones.

Rong et al. [32] studied the characteristics of $\sum REE$ content in various carbonate cements in the sandstones of the Qianjiadian uranium deposit. They found that both $\sum HREE$ and $\sum LREE$ contents increase gradually from calcite to ankerite to siderite to dolomite. Meanwhile, the carbonate cement types in sandstones from the transition zone are mainly dolomite, ankerite, and calcite [12, 14, 48], while those in sandstones from the oxidation zone are mainly calcite [48]. The total content of carbonate cements in sandstones from the transition and oxidation zones of the Qianjiadian uranium deposit is approximately equal [48]. As a result, the relative enrichment degree of HREEs in the transition zone is much higher than that in the oxidation zone, and there is a positive correlation between $\sum HREE$ content and U content. Additionally, dolomite cement is distinguished by its enrichment of HREEs and depletion of LREEs, while calcite cement is characterized by a flat distribution of HREEs and enrichment of LREEs in the sandstones of the Qianjiadian uranium deposit [32]. Therefore, the reduction zone-normalized REE distribution pattern of sandstones from the oxidation zone is right-leaning, while that of sandstones from the transition zone is left-leaning (as shown in Figure 7).

In the interstratified oxidized zone of the Yaojia Formation, the values of δEu in sandstones from the oxidation zone, metallogenic transition zone, and reduction zone are essentially identical and clearly negative (as shown in Table S2 and Figure 4). This indicates that water-rock interaction in sedimentary rocks has limited influence on δEu and that ore-forming fluids were not affected by

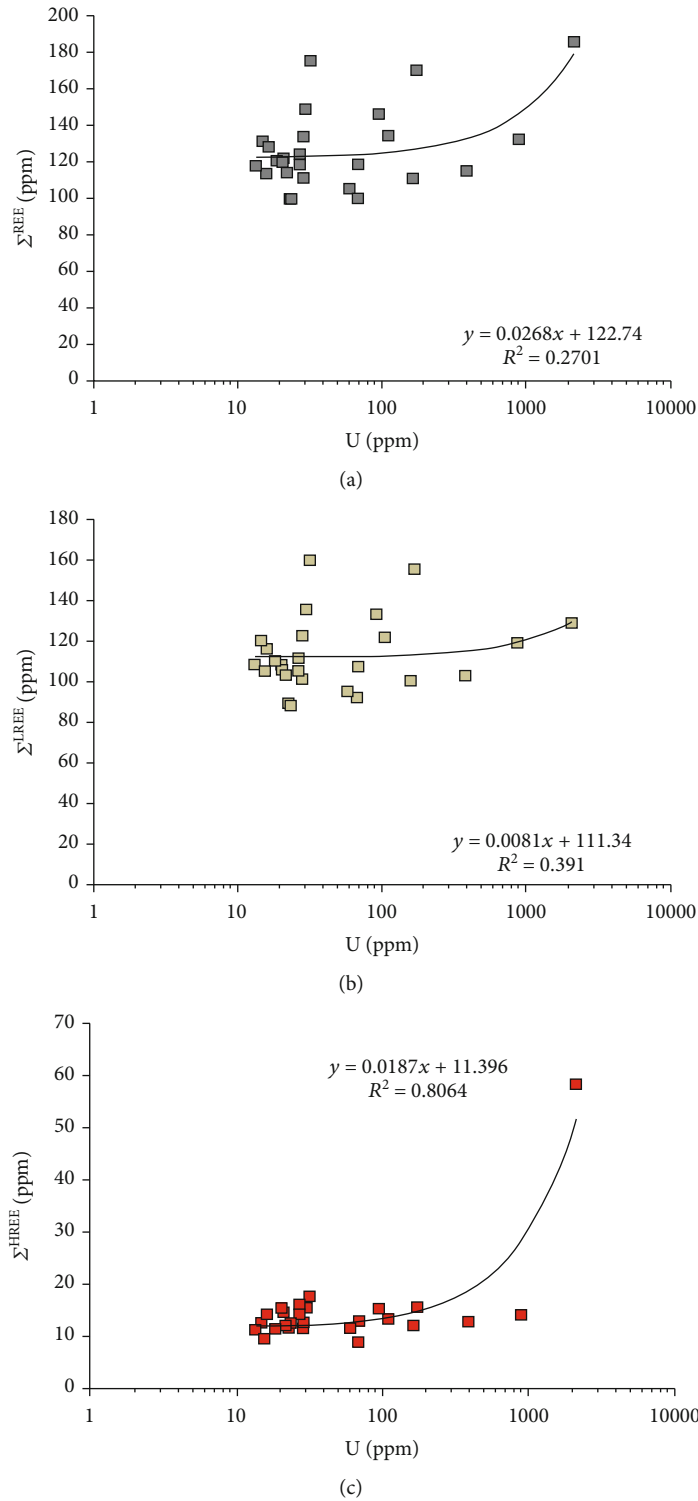


FIGURE 6: (a) Cross-plot of U content against Σ^{REE} content of the sandstones in the transition zone. (b) Cross-plot of U content against Σ^{LREE} content of the sandstones in the transition zone. (c) Cross-plot of U content against Σ^{HREE} content of the sandstones in the transition zone.

hydrothermal fluids from the deep crust. The Eu anomalies here are inherited from the source rocks of the provenance and reflect that the parent rocks in the source areas are mainly composed of felsic rock assemblages.

5.3. Implications for Uranium Mineralization. The formation of the Qianjiadian sandstone-hosted uranium deposit in the Yaojia Formation is generally believed to be closely related to large-scale interstratified oxygenation caused by

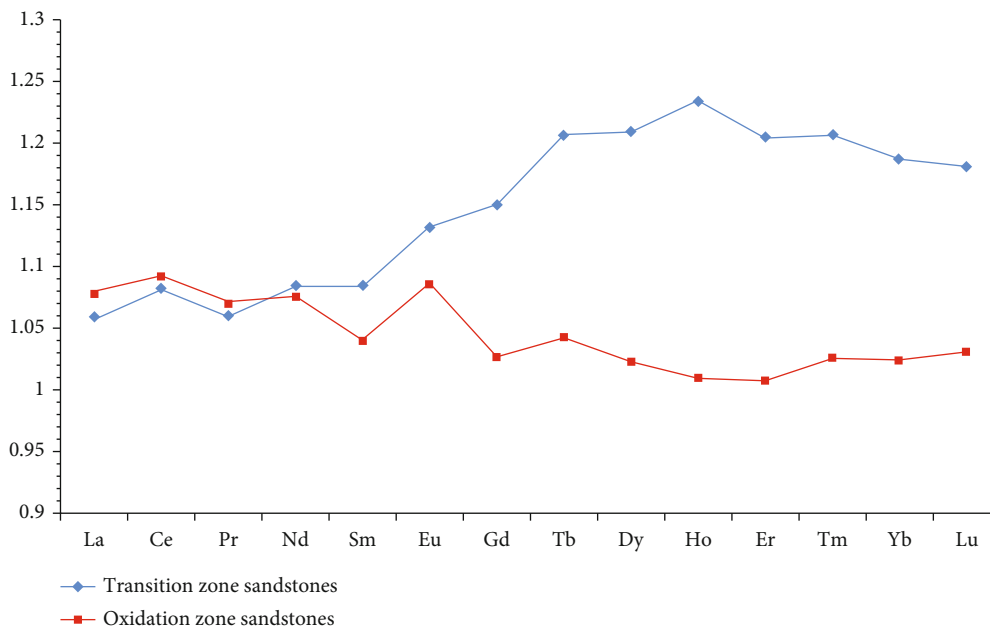


FIGURE 7: Reduction zone-normalized REE patterns of the sandstones in the transition zone and oxidation zone within the Qianjiadian uranium deposit.

oxygenated ore-forming fluids from the southwestern margin of the basin [3, 4, 5–7]. Uranium mineralization mainly occurs in the transition zone near the front of the oxidation zone [3, 5, 7].

There are two main sources of uranium for the mineralization of the Qianjiadian uranium deposit. The first source is the pre-enriched U element in the sandstones of the Yaojia Formation during synsedimentary and early diagenesis. This uranium mainly exists within the clay matrix, Fe-Ti oxides, and uranium-rich lithic fragments such as granite, rhyolite, gneiss, and andesite [1, 13, 15]. This study has shown that 20.33% of the pre-enriched uranium in the sandstones of the oxidation zone was leached and infiltrated into the transition zone by oxygenated groundwater. However, the enrichment degree of uranium in sandstones from the transition zone (with an enrichment coefficient of 48.52) was much higher than the depletion degree of U element in sandstones from the oxidation zone (with an enrichment coefficient of 0.80). Therefore, it can be inferred that the uranium for mineralization in sandstones from the transition zone mainly came from another source.

The second source of uranium was intermediate to felsic volcanic rocks, granites, and gneisses in the southwestern provenance areas of the basin. The structural inversions of the southern Songliao Basin during the Late Cretaceous–Early Paleogene (~70–52 Ma) and Oligo-Miocene (~38–10 Ma) may offer favorable conditions for the formation of the Qianjiadian sandstone-hosted uranium deposit [35, 58, 59]. The structural inversion activities gave rise to the uplift and tilt of the Yaojia Formation in the basin marginal areas. At the same time, uranium-rich source rocks underwent strong weathering, and uranium was leached out in hexavalent form, such as UO_2^{2+} or $[\text{UO}_2(\text{CO}_3)_2]^{2-}$, by oxygenated meteoric fluids under weakly acidic or neutral

conditions. Additionally, certain amounts of Mo, Cd, V, Co, Ni, and Zn elements and REEs were also taken into oxygenated meteoric fluids in the form of MoO_4^{2-} , Cd^{2+} , VO_4^{3-} , Co^{2+} or CoCl^+ , Ni^{2+} or NiCl^+ , Zn^{2+} or ZnCl^+ , and $[\text{REE}(\text{CO}_3)_2]^-$, respectively. The oxygenated ore-forming fluids then permeated into the sandstone layers of the Yaojia Formation. Subsequently, on one hand, the oxygenated ore-forming fluids activated and mobilized the synsedimentary uranium in the host sandstones of the oxidation zone. On the other hand, a small amount of Mo and V elements from the oxygenated ore-forming fluids were absorbed by the iron and manganese hydroxides in the sandstones of the oxide zone. Additionally, some REEs and Cd elements precipitated along with the cementation of carbonates such as calcite and siderite.

In the transition zone of the Qianjiadian uranium deposit, where the dissolved oxygen in the ore-forming fluids was gradually consumed and hydrocarbons were continually injected, sulfates were reduced to sulfides such as pyrite (FeS_2) or greenockite (CdS), and U(VI) was reduced to U(IV), resulting in the precipitation of uranium minerals like pitchblende and coffinite [1, 6, 14], along with the reduction of V(V) to V(III). At the same time, the oxidation of hydrocarbons generated a large amount of CO_2 , which was expected to participate in carbonate cementation [13]. During this process, MoO_4^{2-} from the ore-forming fluids was likely to be transformed into $\text{Mo}(\text{O}_x, \text{S}_{4-x})^{2-}$, which further precipitated by combining with sulfide [46]. A small amount of Cd^{2+} may have precipitated as otavite (CdCO_3) associated with siderite. REEs were likely to enter the mineral lattice of carbonate cement, with $\sum \text{REE}$ content gradually increasing from calcite to ankerite to siderite to dolomite [32]. Co^{2+} , Ni^{2+} , and Zn^{2+} were likely to form insoluble sulfides and enter pyrite as a solid solution [54].

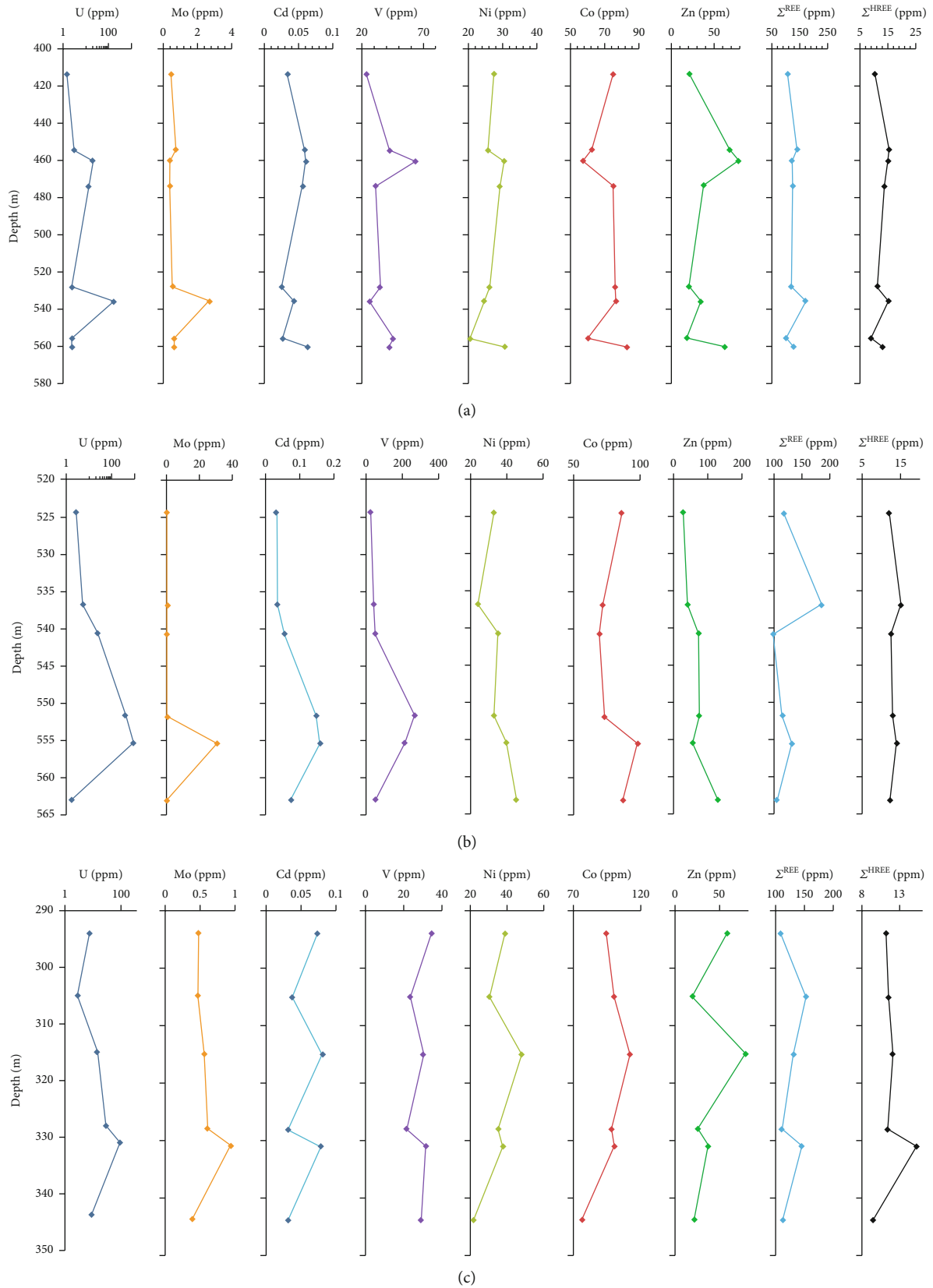


FIGURE 8: (a) Cross-plot of the depth against the element content of the sandstone in the drill hole D80-8. (b) Cross-plot of the depth against the element content of the sandstone in the drill hole D56-0. (c) Cross-plot of the depth against the element content of the sandstone in the drill hole V5-20.

In the sandstones of the transition zone, there is a positive correlation between U content and Mo content, Cr content, V content, and \sum HREE content. The general trend observed is an increase in Mo content, Cd content, V content, or \sum HREE content as U content increases (as shown in Figures 5(a)–5(c) and 6(c)). There is a weak correlation between U content and \sum REE content, with a correlation coefficient of 0.27 (as shown in Figure 6(a)). U content is rarely correlated with Co content, Ni content, Zn content, and \sum LREE content (as shown in Figures 5(e)–5(g)). Three drill holes (D80-8, D56-0, and V5-20) with continuous sampling were selected for a longitudinal comparative study of the evolution characteristics of trace element content, \sum REE content, and uranium content. Cross-plots of depth against element content in the sandstones from the same drill hole show that the variation trend of Mo, Cd, V, Co, Ni, Zn, \sum REE, and \sum HREE contents is consistent with that of U content (as shown in Figure 8). This suggests that the enrichment of Mo, Cd, V, and HREEs is closely associated with uranium mineralization in the Yaojia Formation and can serve as new prospecting indicators for the Qianjiadian uranium deposit.

6. Conclusions

Different trace elements and REEs have varying redox sensitivities and exhibit different valence states and solubility in different redox zones. Trace elements migrate along the redox gradient and redistribute in sedimentary rocks to achieve enrichment or depletion.

- (1) The differentiation characteristics of trace elements and REEs in sandstones from each subzone of the Yaojia Formation in the Qianjiadian uranium deposit are closely related to the geological process of interstratified oxygenation. Oxygenated fluids from the provenance areas, carrying multiple trace elements and REEs, infiltrated the interstratified oxidized zone. About 20.33% of the preexisting uranium in sandstones from the oxidation zone was continuously extracted and entered into the oxygenated ore-forming fluids. In the transition zone, where dissolved oxygen had been exhausted and hydrocarbons had been continuously injected, the Eh value decreased, and pH value increased. U, Mo, Cd, V, Co, Ni, Zn, and HREE were unloaded and precipitated as uranium minerals, sulfide minerals, and carbonate minerals
- (2) Compared to sandstones from the oxidation and reduction zones, sandstones from the transition zone are highly enriched in U; moderately enriched in Mo, Cd, and V; and weakly enriched in Co, Ni, and Zn. In sandstones from the transition zone, U content is positively correlated with Mo content, Cd content, and V content and is rarely correlated with Co content, Ni content, and Zn content
- (3) Compared to sandstones from the reduction zone, both \sum LREE and \sum HREE contents increased in

sandstones from the oxidation and transition zones. Sandstones from the oxidation zone were characterized by the enrichment of LREEs and a flat distribution of HREEs, while sandstones from the transition zone were distinguished by the enrichment of HREEs and a flat distribution of LREEs. In sandstones from the transition zone, U content is positively correlated with \sum HREE content and weakly correlated with \sum REE content

- (4) The enrichment of Mo, Cd, V, and HREEs in sandstones can serve as new prospecting indicators for the Qianjiadian uranium deposit

Data Availability

The data of trace element and REE contents used to support the finding of this study are available from the corresponding author upon request.

Conflicts of Interest

The authors declare that they have no conflicts of interest.

Acknowledgments

This research was supported financially by the National Natural Science Foundation of China (grant number 42072099), the science and technology research project of Education Department of Jiangxi Province (grant number GJJ201130), the Open Foundation of Fundamental Science on Radioactive Geology and Exploration Technology Laboratory (grant number 2022RGET06), and the Scientific Research Foundation for PhD, East China University of Technology (grant number DHBK2018028).

Supplementary Materials

Table S1: trace element contents (ppm) of sandstones in the Qianjiadian uranium deposit. Table S2: rare earth element contents (ppm) and associated geochemical parameters for sandstones in the Qianjiadian uranium deposit. (*Supplementary Materials*)

References

- [1] C. Bonnetti, X. Liu, Z. Yan et al., “Coupled uranium mineralisation and bacterial sulphate reduction for the genesis of the Baxingtuo sandstone-hosted U deposit, SW Songliao Basin, NE China,” *Ore Geology Reviews*, vol. 82, no. 108–129, pp. 108–129, 2017.
- [2] R. Reynolds, M. Goldhaber, and D. Carpenter, “Biogenic and nonbiogenic ore-forming processes in the South Texas uranium district; evidence from the Panna Maria deposit,” *Economic Geology*, vol. 77, no. 3, pp. 541–556, 1982.
- [3] Q. Pang, X. Chen, X. Fang, and Y. Sun, “Discussion on the interlayer oxidation and uranium metallogenesis in Qianjiadian uranium deposit, Songliao Basin,” *Uranium Geology*, vol. 26, no. 1, pp. 9–23, 2010.

- [4] J. Zheng, "Geological setting and exploration potential of Qianjiadian uranium deposit in Kailu basin," *Uranium Geology*, vol. 26, no. 4, pp. 193–200, 2010.
- [5] J. Cai, Z. Yan, L. Zhang et al., "Relationship between grey sandstone and uranium mineralization in Yaojia Formation of Upper Cretaceous in Tongliao, Inner Mongolia," *Journal of East China University of Technology (Natural Science)*, vol. 41, no. 4, pp. 328–335, 2018.
- [6] H. Rong, Y. Jiao, L. Wu et al., "Origin of the carbonaceous debris and its implication for mineralization within the Qianjiadian uranium deposit, southern Songliao Basin," *Ore Geology Reviews*, vol. 107, pp. 336–352, 2019.
- [7] M. Cao, H. Rong, Z. Chen et al., "Quantitative characterization and controlling factors of the interlayer oxidation zone of Qianjiadian uranium deposit, Songliao Basin," *Earth Science*, vol. 46, no. 10, pp. 3453–3466, 2021.
- [8] X. Chen, W. Xiang, T. Li et al., "Distribution characteristics of interlayer oxidation zone and its relationship with sedimentary facies and uranium mineralization in QJD uranium deposit, Songliao Basin, NE China," *World Nuclear Geoscience*, vol. 23, no. 3, pp. 137–144, 2006.
- [9] Y. Luo, H. Ma, Y. Xia, and Z. Zhang, "Geologic characteristics and metallogenic model of Qianjiadian uranium deposit in Songliao basin," *Uranium Geology*, vol. 23, no. 4, pp. 193–200, 2007.
- [10] Y. Luo, Z. He, H. Ma, and X. Sun, "Metallogenic characteristics of Qianjiadian sandstone uranium deposit in Songliao basin," *Mineral Deposits*, vol. 31, no. 2, pp. 391–400, 2012.
- [11] Z. Zhao, G. Liu, and C. Cui, "The prospecting direction for sandstone type uranium deposit in interlayered oxidation zone in the southwest of Songliao Basin," *Bulletin of Mineralogy, Petrology and Geochemistry*, vol. 17, no. 3, pp. 156–159, 1998.
- [12] F. Nie, Z. Yan, F. Xia et al., "Hot fluids flows in the sandstone-type uranium deposit in the Kailu Basin, Northeast China," *Geological Bulletin of China*, vol. 36, no. 10, pp. 1850–1866, 2017.
- [13] L. Zhao, C. Cai, R. Jin et al., "Mineralogical and geochemical evidence for biogenic and petroleum-related uranium mineralization in the Qianjiadian deposit, NE China," *Ore Geology Reviews*, vol. 101, pp. 273–292, 2018.
- [14] B. Song, H. Sun, S. Yang et al., "Characteristics and uranium mineralization of ore-bearing rock series in Qianjiadian sandstone-type uranium deposits, Songliao Basin," *Journal of Palaeogeography (Chinese Edition)*, vol. 22, no. 2, pp. 309–320, 2020.
- [15] Z. Shan, A. Lei, B. Song, C. Ao, S. Yang, and H. Han, "Features of clay minerals in the Upper Cretaceous Yaojia Formation sandstones of the Qianjiadian area in the Songliao Basin and its relation to uranium mineralization," *Geology in China*, vol. 49, no. 1, pp. 271–283, 2022.
- [16] Y. Xia, J. Zheng, Z. Li, L. Li, and S. Tian, "Metallogenic characteristics and metallogenic model of Qianjiadian uranium deposit in Songliao Basin," *Mineral Deposits*, vol. 29, no. S1, pp. 154–155, 2010.
- [17] Z. Wu, X. Han, and H. Hu, "Sedimentary tectonic evolution and uranium mineralization of post Late Cretaceous in Shaogen area of Lujiapu sag, Kailu Basin," *Acta Sedimentologica Sinica*, vol. 36, no. 1, pp. 20–32, 2018.
- [18] F. Xia, Y. Jiao, H. Rong, L. Wu, Q. Zhu, and L. Wan, "Geochemical characteristics and geological implications of sandstones from the Yaojia Formation in Qianjiadian Uranium Deposit, southern Songliao Basin," *Earth Science*, vol. 44, no. 12, pp. 4235–4251, 2019.
- [19] Z. Xu, B. Zhang, H. Li et al., "Geochemistry of the Yaojia Formation sandstone in the Kailu Depression, Songliao Basin: implications for its provenance and tectonic setting," *Bulletin of Mineralogy, Petrology and Geochemistry*, vol. 38, no. 3, pp. 572–586, 2019.
- [20] C. Deng, H. He, Y. Pan, and R. Zhu, "Chronology of the terrestrial Upper Cretaceous in the Songliao Basin, Northeast Asia," *Palaeogeography, Palaeoclimatology, Palaeoecology*, vol. 385, no. 1, pp. 44–54, 2013.
- [21] J. Liu, M. Qin, Y. Cai, Z. Liu, Z. Zhang, and L. Yao, "Late Mesozoic tectonic evolution of the southern Great Xing'an Range, northeastern China: constraints from detrital zircon U–Pb and Hf isotopes of Late Cretaceous sandstones in the southwestern Songliao Basin," *Geological Journal*, vol. 55, no. 6, pp. 4415–4425, 2020.
- [22] G. Zhu, S. Zhang, B. Katz et al., "Geochemical features and origin of natural gas in heavy oil area of the Western Slope, Songliao Basin, China," *Geochemistry*, vol. 74, no. 1, pp. 63–75, 2014.
- [23] Z. Feng, C. Jia, X. Xie, S. Zhang, Z. Feng, and T. Cross, "Tectonostratigraphic units and stratigraphic sequences of the non-marine Songliao basin, Northeast China," *Basin Research*, vol. 22, no. 1, pp. 79–95, 2010.
- [24] P. Wang, W. Liu, S. Wang, and W. Song, " $^{40}\text{Ar}/^{39}\text{Ar}$ and K/Ar dating on the volcanic rocks in the Songliao basin, NE China: constraints on stratigraphy and basin dynamics," *International Journal of Earth Sciences*, vol. 91, no. 2, pp. 331–340, 2002.
- [25] X. Du, X. Xie, Y. Lu et al., "Distribution of continental red paleosols and their forming mechanisms in the late cretaceous Yaojia formation of the Songliao Basin, NE China," *Cretaceous Research*, vol. 32, no. 2, pp. 244–257, 2011.
- [26] S. Li, F. Chen, W. Siebel et al., "Late Mesozoic tectonic evolution of the Songliao basin, NE China: evidence from detrital zircon ages and Sr–Nd isotopes," *Gondwana Research*, vol. 22, no. 3–4, pp. 943–955, 2012.
- [27] M. Cao, "Constraints of the sequence stratigraphic structure of uranium-bearing series on mineralization in Qianjiadian uranium deposit, Songliao Basin," *Bulletin of Geological Science and Technology*, vol. 40, no. 4, pp. 131–142, 2021.
- [28] Y. Song, J. Ren, H. Yang, D. Tong, and C. Lei, "Characteristics and dynamic background of bottom boundary in Yaojia Formation of the northern Songliao Basin," *Acta Petrolei Sinica*, vol. 31, pp. 187–195, 2010.
- [29] H. Rong, Y. Jiao, L. Wu et al., "Epigenetic alteration and its constraints on uranium mineralization from the Qianjiadian uranium deposit, southern Songliao Basin," *Earth Science*, vol. 41, no. 1, pp. 153–166, 2016.
- [30] Y. Jiao, L. Wu, Y. Peng et al., "Sedimentary-tectonic setting of the deposition-type uranium deposits forming in the Paleozoic tectonic domain, North China," *Earth Science Frontiers*, vol. 22, no. 1, pp. 189–205, 2015.
- [31] H. Rong, W. Jiao, W. Liu et al., "Influence mechanism of palaeoclimate of uranium-bearing strata on mineralization: a case study from the Qianjiadian sandstone-hosted uranium deposit, Songliao Basin, China," *Ore Geology Reviews*, vol. 138, article 104336, 2021.
- [32] H. Rong, Y. Jiao, X. Liu, L. Wu, J. Jia, and M. Cao, "Effects of basic intrusions on REE mobility of sandstones and their

- geological significance: a case study from the Qianjiadian sandstone-hosted uranium deposit in the Songliao Basin," *Applied Geochemistry*, vol. 120, article 104665, 2020.
- [33] Y. Song, A. Stepashko, K. Liu et al., "Post-rift tectonic history of the Songliao Basin, NE China: cooling events and post-rift unconformities driven by orogenic pulses from plate boundaries," *Journal of Geophysical Research: Solid Earth*, vol. 123, no. 3, pp. 2363–2395, 2018.
- [34] S. Wang, Y. Cheng, L. Zeng et al., "Thermal imprints of Cenozoic tectonic evolution in the Songliao Basin, NE China: evidence from apatite fission-track (AFT) of CCSD-SK1 borehole," *Journal of Asian Earth Sciences*, vol. 195, article 104353, 2020.
- [35] Y. Cheng, S. Wang, T. Zhang et al., "Regional sandstone-type uranium mineralization rooted in Oligo-Miocene tectonic inversion in the Songliao Basin, NE China," *Gondwana Research*, vol. 88, pp. 88–105, 2020.
- [36] Y. Zhang, Z. Liao, Z. Wu et al., "Climate change controls on extreme organic matter enrichment in Late Permian marine-terrestrial transitional shales in Guizhou, South China," *Journal of Petroleum Science and Engineering*, vol. 218, article 111062, 2022.
- [37] H. Ji, H. Tao, Q. Wang, D. Ma, and L. Hao, "Petrography, geochemistry, and geochronology of lower Jurassic sedimentary rocks from the northern Tianshan (West Bogda area), Northwest China: implications for provenance and tectonic evolution," *Geological Journal*, vol. 54, no. 3, pp. 1688–1714, 2019.
- [38] D. Piper and R. Perkins, "A modern vs. Permian black shale—the hydrography, primary productivity, and water-column chemistry of deposition," *Chemical Geology*, vol. 206, no. 3–4, pp. 177–197, 2004.
- [39] W. Boynton, "Cosmochemistry of the rare earth elements: meteorite studies," *Developments in Geochemistry*, vol. 2, pp. 63–114, 1984.
- [40] R. Sani, B. Peyton, J. Amonette, and G. Geesey, "Reduction of uranium(VI) under sulfate-reducing conditions in the presence of Fe(III)-(hydr)oxides¹," *Geochimica et Cosmochimica Acta*, vol. 68, no. 12, pp. 2639–2648, 2004.
- [41] J. Mcmanus, W. Berelson, G. Klinkhammer, D. Hammond, and C. Holm, "Authigenic uranium: relationship to oxygen penetration depth and organic carbon rain," *Geochimica et Cosmochimica Acta*, vol. 69, no. 1, pp. 95–108, 2005.
- [42] D. Brookins, *Eh-pH Diagrams for Geochemistry*, Springer Science & Business Media, 2012.
- [43] H. Brumsack, "Geochemistry of recent TOC-rich sediments from the Gulf of California and the Black Sea," *Geologische Rundschau*, vol. 78, no. 3, pp. 851–882, 1989.
- [44] J. Crusius, S. Calvert, T. Pedersen, and D. Sage, "Rhenium and molybdenum enrichments in sediments as indicators of oxic, suboxic and sulfidic conditions of deposition," *Earth and Planetary Science Letters*, vol. 145, no. 1–4, pp. 65–78, 1996.
- [45] B. Erickson and G. Helz, "Molybdenum(VI) speciation in sulfidic waters: stability and lability of thiomolybdates," *Geochimica et Cosmochimica Acta*, vol. 64, no. 7, pp. 1149–1158, 2000.
- [46] T. Vorlicek, M. Kahn, Y. Kasuya, and G. Helz, "Capture of molybdenum in pyrite-forming sediments: role of ligand-induced reduction by polysulfides¹," *Geochimica et Cosmochimica Acta*, vol. 68, no. 3, pp. 547–556, 2004.
- [47] G. Tu, Z. Gao, and R. Zhong, *Geochemistry and Metallogenic Mechanism of Dispersed Elements*, Geological Publishing House, 2004.
- [48] J. Jia, H. Rong, Y. Jiao et al., "Occurrence of carbonate cements and relationship between carbonate cementation and uranium mineralization of Qianjiadian uranium deposit, Songliao Basin," *Earth Science*, vol. 43, no. S2, pp. 149–161, 2018.
- [49] R. Wanty and M. Goldhaber, "Thermodynamics and kinetics of reactions involving vanadium in natural systems: accumulation of vanadium in sedimentary rocks," *Geochimica et Cosmochimica Acta*, vol. 56, no. 4, pp. 1471–1483, 1992.
- [50] J. Morford and S. Emerson, "The geochemistry of redox sensitive trace metals in sediments," *Geochimica et Cosmochimica Acta*, vol. 63, no. 11–12, pp. 1735–1750, 1999.
- [51] S. Yang, "Geochemical characteristics of interlayer oxidation zone in Qianjiadian sandstone-type uranium deposits, Songliao Basin," *Journal of Palaeogeography (Chinese Edition)*, vol. 22, no. 2, pp. 321–332, 2020.
- [52] G. Breit and R. Wanty, "Vanadium accumulation in carbonaceous rocks: a review of geochemical controls during deposition and diagenesis," *Chemical Geology*, vol. 91, no. 2, pp. 83–97, 1991.
- [53] J. Morse and K. Emeis, "Carbon/sulphur/iron relationships in upwelling sediments," *Geological Society London Special Publications*, vol. 64, no. 1, pp. 247–255, 1992.
- [54] N. Tribouillard, T. Algeo, T. Lyons, and A. Riboulleau, "Trace metals as paleoredox and paleoproductivity proxies: an update," *Chemical Geology*, vol. 232, no. 1–2, pp. 12–32, 2006.
- [55] B. Lottermoser, "Rare-earth element behaviour associated with strata-bound scheelite mineralisation (Broken Hill, Australia)," *Chemical Geology*, vol. 78, no. 2, pp. 119–134, 1989.
- [56] A. Michard, "Rare earth element systematics in hydrothermal fluids," *Geochimica et Cosmochimica Acta*, vol. 53, no. 3, pp. 745–750, 1989.
- [57] A. Michard and F. Albarède, "The REE content of some hydrothermal fluids," *Chemical Geology*, vol. 55, no. 1–2, pp. 51–60, 1986.
- [58] Y. Cheng, S. Wang, Y. Li et al., "Late Cretaceous–Cenozoic thermochronology in the southern Songliao Basin, NE China: new insights from apatite and zircon fission track analysis," *Journal of Asian Earth Sciences*, vol. 160, pp. 95–106, 2018.
- [59] Y. Cheng, S. Wang, R. Jin, J. Li, C. Ao, and X. Teng, "Global Miocene tectonics and regional sandstone-style uranium mineralization," *Ore Geology Reviews*, vol. 106, pp. 238–250, 2019.